*Published online 1 August 2013*

*Nucleic Acids Research, 2013, Vol. 41, No. 17* ***e168***
*doi:10.1093/nar/gkt668*

# A multidimensional platform for the purification of non-coding RNA species

**Yok Hian Chionh[1,2], Chia-Hua Ho[1], Dumnoensun Pruksakorn[3,4], I. Ramesh Babu[3], Chee Sheng Ng[1,5], Fabian Hia[1], Megan E. McBee[3], Dan Su[3], Yan Ling Joy Pang[3], Chen Gu[3], Hongping Dong[7], Erin G. Prestwich[3], Pei-Yong Shi[7], Peter Rainer Preiser[1,5], Sylvie Alonso[1,2,6] and Peter C. Dedon[1,3,*]**

[1]Singapore-MIT Alliance for Research and Technology, Infectious Disease Interdisciplinary Research Group, Campus for Research Excellence and Technological Enterprise, Singapore 138602, [2]Department of Microbiology, Yong Loo Lin School of Medicine, National University of Singapore, Singapore 117597, [3]Department of Biological Engineering and Center for Environmental Health Sciences, Massachusetts Institute of Technology, Cambridge, MA 02139, USA, [4]Applied Biological Science Program, Chulabhorn Graduate Institute, Bangkok 10210, Thailand, [5]Division of Molecular Genetics & Cell Biology, School of Biological Sciences, Nanyang Technological University, Singapore 637551, [6]Immunology Programme, Life Science Institute, Centre for Life Science, Singapore 117456 and [7]Novartis Institute for Tropical Disease, Singapore 138670

Received April 22, 2013; Revised July 7, 2013; Accepted July 8, 2013

## ABSTRACT

**A renewed interest in non-coding RNA (ncRNA) has led to the discovery of novel RNA species and post-transcriptional ribonucleoside modifications, and an emerging appreciation for the role of ncRNA in RNA epigenetics. Although much can be learned by amplification-based analysis of ncRNA sequence and quantity, there is a significant need for direct analysis of RNA, which has led to numerous methods for purification of specific ncRNA molecules. However, no single method allows purification of the full range of cellular ncRNA species. To this end, we developed a multidimensional chromatographic platform to resolve, isolate and quantify all canonical ncRNAs in a single sample of cells or tissue, as well as novel ncRNA species. The applicability of the platform is demonstrated in analyses of ncRNA from bacteria, human cells and plasmodium-infected reticulocytes, as well as a viral RNA genome. Among the many potential applications of this platform are a system-level analysis of the dozens of modified ribonucleosides in ncRNA, characterization of novel long ncRNA species, enhanced detection of rare transcript variants and analysis of viral genomes.**

## INTRODUCTION

The renewed interest in RNA modifications and the discovery of many new non-coding RNA (ncRNA) species (1–5) has increased the demand for methods to purify RNA species. However, although eukaryotic mRNA is readily purified by exploiting a polyA tail, studies of ncRNA structure and biochemistry, post-transcriptional processing (capping, end-processing), ribonucleoside modification and biological function have been limited by the inability to obtain RNA in pure form (6–11). This is especially important given the emerging interest in studying RNA biology on a systems level, with coordinated analysis of modified ribonucleosides present in virtually all forms of RNA (4,5,12,13). Existing RNA purification methods are limited by specificity, size range or yield. Although affinity purification approaches are specific to a unique sequence, more general size-based gel electrophoretic approaches are hampered by a narrow size range, gel contaminants from RNA elution and high losses during purification (14–16). Liquid chromatography (LC) approaches using all types of stationary phase have solved some of these problems, with a wider size range but lower resolving power than gel electrophoresis (17–22). Improvements in capacity and specificity have been achieved by specialized combinations of chromatography with affinity purification (23,24) and electrophoresis (25). Though useful for

*To whom correspondence should be addressed. Tel: +1 617 253 8017; Fax: +1 617 324 7554; Email: pcdedon@mit.edu
Present address:
Dumnoensun Pruksakorn, Department of Orthopedics, Faculty of Medicine, Chiang Mai University, Tambon Sriphum, Chiang Mai 50200, Thailand.

isolating specific RNA classes or RNA species, these methods do not permit size fractionation of total RNA or isolation of all classes of ncRNA from single sample for a system-level analysis of modified ribonucleosides, for example.

To address this unmet need in RNA biology, we report a comprehensive multidimensional high-performance liquid chromatography (HPLC) platform that can be used to purify all major classes of ncRNA from a single sample of total RNA. The method takes advantage of the strengths of two types of HPLC, thus increasing the peak capacity and the resolution of ncRNA across a wide size range. Such an approach is well developed in proteomics and has proven valuable in fractionating complex biological mixtures (26,27). To resolve ncRNA, we combined two ranges of size-exclusion chromatography (SEC) with ion-pair reverse-phase chromatography (IP RPC) to achieve a complete separation of RNA species ranging from 20 to >10 000 nucleotides (nt), including viral RNA genomes, large and small subunit rRNAs, tRNA and miRNA. The approach is demonstrated for both individual HPLC steps (1D) and for 2D HPLC resolution of total RNA from human plasmodium parasite and bacterial cells, as well as a dengue viral RNA genome.

## MATERIALS AND METHODS

### Chemicals and reagents

RPMI 1640, fetal bovine serum and Penicillin Streptomycin (Pen-Strep) for cell cultures were purchased from Gibco, Invitrogen (Carlsbad, CA). RiboGreen and PicoGreen kits for RNA and DNA quantitation, respectively, were purchased from Molecular Probes, Invitrogen (Eugene, OR). Chemicals unless otherwise specified were purchased from Sigma Chemical Co. (St. Louis, MO).

### Bacterial and mammalian cell culture

*Escherichia coli* strain DH5α was grown for 3 h in Luria-Bertani medium (Becton, Dickinson and Company, Franklin Lakes, NJ) at 37°C with shaking (250 rpm) until an optical density (600 nm; OD600) of 0.6 was reached at mid-exponential growth phase. *Mycobacterium bovis* Bacille Calmette-Guérin (BCG) strain Pasteur 1173P2 bacilli (ATCC) were grown in 7H9 culture media (4.9 g of 7H9 powder, 10 ml of 50% glycerol, 2.5 ml of 20% TWEEN 80, 900 ml of water and 100 ml of ADS solution) at 37°C in an 850 $cm^2$ polystyrene roller bottle (Corning, NY, USA) at 10 rpm to an OD600 = 0.6, at which point the concentration of cells was $\sim 5 \times 10^7$/ml. Mononuclear, B lymphoblastoid CCRF-SB and TK6 cells (ATCC) were grown in suspension cultures in RPMI complete medium (90% RPMI 1640 medium, 10% fetal bovine serum with added Pen-Strep) to a density of $10^7$ cells/ml.

### *In vitro* transcription of dengue viral RNA from plasmid DNA template

Genome-length 10.7 kb viral RNA (vRNA) of dengue viral 1 (DENV-1) was *in vitro* transcribed from full-length cDNA plasmid linearized by *SacII* (28). The vector was then electroporated into BHK-21 cells and transfected cells resuspended in 20 ml of DMEM medium (29). The transfected cultures were subsequently subjected to viral production and specific infectivity assays as communicated previously (28). RNA was isolated with Trizol reagent (Invitrogen) as directed by the manufacturer and re-purified on an Agilent Bio SEC-5 2000 Å (i.d. 7.8 mm; length 300 mm) column (Agilent Technologies, Foster City, CA) with an isocratic elusion as described below.

### Rodent infection with *Plasmodium berghei* and isolation of schizont-infected murine reticulocytes

Male BALB/c mice and male WISTAR rats, 6–8 weeks old, were obtained from Sembawang Laboratory Animal Center, National University of Singapore, and subsequently bred under specific pathogen-free conditions at Nanyang Technological University Animal Holding Unit. Infection and handling of laboratory animals with the blood-stage *P. berghei* ANKA strain were performed using the methods described elsewhere (30). Blood was collected from infected rats at a parasitemia of 1–3% by cardiac puncture with heparin (Sigma). Blood was then filtered by leukocyte filter (Plasmodipur filter, EuroDiagnostica) and cultured until the schizont stage in complete RPMI 1640 containing 20% FBS with gentle shaking at 37°C. Schizont-infected cells were separated from uninfected cells by 50–60% Nycodenz (Sigma-Aldrich) gradient centrifugation. Schizonts were purified by lysing rat erythrocytes with 0.15% saponin and washed three times with cold phosphate buffered saline (PBS) before flash freezing in liquid nitrogen.

### Ethics statement

The study was carried out in strict accordance with the recommendations of the National Advisory Committee for Laboratory Animal Research guidelines under the Animal and Birds (Care and Use of Animals for Scientific Purposes) Rules of Singapore. The protocol was approved by the Institutional Animal Care and Use Committee of the Nanyang Technological University of Singapore (Approval number: ARFSBS/NIE A002). All efforts were made to minimize the suffering.

### Total RNA extraction

Before lysis, cells were washed with ice-cold PBS again. BCG pellets were lysed by French high-pressure homogenization (Thermo Scientific). Ice-cold phenol:chloroform:isoamyl alcohol (25:24:1) was added directly to the lysate and total RNA obtained with PureLink miRNA Isolation Kit (Invitrogen), as described by the manufacturer. For *E. coli*, the lysis was performed with 100 µl of lysozyme (1 mg/ml) for 20 min at ambient temperature. For *E. coli*, total RNA was extracted with Trizol reagent (Invitrogen), precipitated with ice-cold isopropyl alcohol and washed with 75% ethanol. CCRF-SB, TK6 and *P. berghei*-infected reticulocytes were directly lysed in Trizol reagent and eukaryotic total RNA extracted in an identical fashion. RNA pellets were air-dried and

re-dissolved in RNAse-free water. DNase I (Qiagen, Valencia, CA) treatment was performed for 15 min at 37°C. The quality and quantity of RNA was determined using Agilent Bioanalyzer RNA 6000 Nano Chips (Agilent Technologies, Santa Clara, CA). Only samples with an RNA integrity number of ≥8.0 were used for further experiments.

### Size-exclusion chromatography of total RNA

The 1D SEC was performed with either a Bio SEC-3 300 Å (i.d. 7.8 mm; length 300 mm) or a Bio SEC-5 1000 Å (i.d. 7.8 mm; length 300 mm) column (Agilent Technologies, Foster City, CA), with 100 mM ammonium acetate (pH 7.0) as the mobile phase. Isocratic separations were performed at 1 ml/min for 20 min under partially denaturing conditions at 60°C on the Agilent 1200 HPLC system. The 2D SEC was performed with Bio SEC-3 300 Å and with either Bio SEC-5 1000 Å or Bio SEC-5 2000 Å (id 7.8 mm, length 300 mm) columns. A second Agilent 1260 Infinity system is connected with the valve configuration described in Supplementary Figure S2, and isocratic separations were performed with 100 mM ammonium acetate at 0.5 ml/min rates for 40 min at 60°C. Chromatograms were recorded at every 10 nm from 200 to 300 nm. Peaks were collected with an Agilent 1260 Infinity auto-sampler by time segments. For separations of BCG total RNA, a Bio SEC-5 1000 Å column was connected to the column 1 position, whereas a Bio SEC-3 300 Å column was connected to the column 2 position. From 0–0.1 min, column 1 was connected to the detector; from 0.1–18.5 min, column 2 was connected and this is switched back to column 1 at 18.5 min. For separations of TK6 total RNA, a Bio SEC-5 2000 Å column was connected to the column 1 position, whereas a Bio SEC-3 300 Å column was connected to the column 2 position. From 0–0.1 min, column 1 is connected to the detector, and from 0.1–20 min, column 2 is connected and switched back to column 1 at 20 min. For separations of total RNA from *P. berghei*-infected rat reticulocytes, a Bio SEC-3 300 Å column was connected to the column 1 position, whereas a Bio SEC-5 1000 Å column was connected to the column 2 position; the column switching scheme was identical as that used for TK6 total RNA. For the analysis of TK6 total RNA, 100 mM triethylammonium acetate (TEAA) (pH 7.0), instead of 100 mM ammonium acetate, was used as the mobile phase. In addition, a Bio SEC-5 2000 Å column was used. All other conditions were kept constant.

### IP RPC of total RNA

CCRF-SB and TK6 total RNA were analyzed by IP RPC on the Agilent 1200 system using a Source 5RPC 4.6/150 column (GE Healthcare Life Sciences, Piscataway, NJ). HPLC was performed using a two eluent buffer system in which buffer A consisted of an aqueous solution of 100 mM TEAA (pH 7.0) with 2% acetonitrile, and buffer B consisted of 100% acetonitrile under partially denaturing conditions at 60°C with chromatograms recorded and as described earlier in the text. IP RPC was performed with the following gradient conditions: flow rate 1 ml/min, 5–5.5% B over 6 min, to 13% B over 45 min, to 16.5% B over 9 min, to 100% B over 10 min, held at 100% B for 10 min, brought back to 5% B over 10 min.

### Analysis of isolated RNA species

The 2D-SEC-purified DENV-1 vRNA (10.7 kb) 28S, and 18S rRNA from CCRF-SB and TK6, 23S and 16S rRNA from *E. coli* and BCG, and *P. berghei* 28S, 18S and 800 nt rRNA were concentrated and desalted with an Amicon Ultracel 10k MWCO spin column (Millipore, Bedford, MA), whereas 5.8S, 5S, tRNA and miRNA from the aforementioned total RNA preparations were concentrated and desalted with a Vivacon-500 2k MWCO spin column (Sartorius, Goettingen, Germany). The efficiency of the isolation process, quality and quantity of each RNA species after HPLC purification and desalting were assessed using the Agilent Bioanalyzer (Agilent). RNA 6000 Pico chips were used to evaluate 28S, 18S, 23S, 16S rRNA and *P. berghei* 800 nt rRNA, whereas 5S, 5.8S rRNA, tRNA and miRNA were evaluated on Small RNA chips. The presence of contaminating DNA was determined using a PicoGreen dye-based quantitation assay, using calf-thymus DNA (Sigma) as a calibration standard.

The theoretical maximum composition of each RNA species from their respective total RNA preparations was estimated by the product of the percentage area under the curve for each chromatographic peak with the quantity of total RNA injected into the chromatographic system. We then established the yields of each RNA species that were recovered from the RNA isolation process by calculating the ratios between the quantities of purified RNA against its corresponding theoretical maximum yield.

### RiboGreen assay for species-specific fluorometric responses

Purified RNA samples were diluted to stock solutions of 20 μg/ml RNA in TE buffer (10 mM Tris, 1 mM EDTA, pH 7.8), and their concentrations were confirmed with a Nanodrop Spectrophotometer (Thermo Scientific, Wilmington, DE). A 96-well-based RiboGreen RNA quantitation assay was performed as indicated by the manufacturer instructions, with the stocks of each purified RNA species used in place of the RNA standard provided. Scans for RiboGreen fluorescence were also performed from 450 to 650 nm at 10 nm intervals. Fluorometric measurements were conducted on a BioTek Synergy 2 Multi-Mode Microplate Reader (Winooski, VT) with 485/20 nm and 528/20 nm bandpass filters for excitation and emission, respectively. All readings were taken at 25°C.

### Detection and relative quantification of ribonucleosides from BCG tRNA by chromatography-coupled mass spectrometry

Purified BCG tRNA (5 μg) from three independent exponentially growing cultures of BCG was hydrolyzed enzymatically as described previously (31). Hydrolyzed

RNA was resolved on a Thermo Hypersil aQ column (100 × 2.1 mm, 1.9 μm particle size) in a two buffer eluent system, with buffer A consisting of water with 0.1% (v/v) formic acid and buffer B consisting of acetonitrile with 0.1% (v/v) formic acid. HPLC was performed at a flow rate of 0.3 ml/min. The gradient of acetonitrile in 0.1% formic acid was as follows: 0–12 min, held at 0%; 12–15.3 min, 0–1%; 15.3–18.7 min, 1–6%; 18.7–20 min, held at 6%; 20–24 min, 6–100%; 24–30 min, held at 100%; 30–35 min, 100–0%; 35–40 min, 0%. The HPLC column was maintained at 25°C and directly connected to an Agilent 6460 triple quadrupole mass spectrometer (LC-MS/MS) with ESI Jetstream ionization operated in positive ion mode. Multiple reaction monitoring was performed to detect and quantify the ribonucleosides with the parameters of retention time, $m/z$ of the transmitted parent ion, and $m/z$ of the monitored product ion as noted in Supplementary Table S2. Fragmentor voltages of 89 V and collision energies of 18 V were used. The dwell time for each ribonucleoside was 100 ms, and 18 ions were monitored from 0.5 to 28 min. The voltages and source gas parameters were as follows: gas temperature, 350°C; gas flow, 5 l/min; nebulizer, 40 psi; sheath gas temperature, 325°C; sheath gas flow, 7 l/min and capillary voltage, 3500 V.

### $MS^2$ Structural characterization of $N^6$,$N^6$-dimethyladenosine in BCG tRNA

The ribonucleoside-like species eluting at 20.14 min and possessing an $[M + H]^+$ ion with $m/z$ of 296.1356 was subjected to structural characterization by collision-induced dissociation performed on an Agilent 6520 Accurate-Mass Quadrupole Time-of-Flight mass spectrometer (LC-Q-TOF) using the same column and chromatographic system as described earlier in the text. The mass spectrometer was operated in positive ion mode with the following voltages and source gas parameters: gas temperature, 325°C; drying gas, 7 l/min; nebulizer, 15 psig; capillary voltage, 4000 V. The $m/z$ detection range for parent ions was 100–800 and that for product ions was 50–500. The fragmentor voltage was set at 85 V and the collision energy was 25 V.

### Data graphing and statistical analysis

Analysis of covariance of RNA species-specific RiboGreen calibration curves was performed with Graphpad Prism 5.0. Multiple regressions were not performed. Instead, relative pair-wise comparisons were made between each purified RNA species and the total RNA from which it was isolated. The 3D and contour plots were made with Matlab R2012a (Mathworks, Natick, MA). Peaks in the raw chromatograms corresponding to miRNA, tRNA, 5S rRNA, sn/snoRNA, 5.8S rRNA, 18S rRNA and 28S rRNA were manually assigned based on their respective sizes as determined by Bioanalyzer 2100 LabChips. In the 3D plot, the region on the X-Y basal plane that represents a particular RNA species was determined by the characteristic retention time of that species in both LC methods; the height of peaks in the Z-direction, each representing a particular RNA species, denotes the geometric average of the absorbance values of that specific RNA in both LC methods, which was calculated as the square root of the product of the two absorbance values. This assignment of $z$-axis values takes into account the absorbance measurements by both LC methods, and therefore accurately reflects the relative intensity or abundance of the different RNA species present within one cellular extract. For all areas on the X-Y basal plane, other than those designated with a particular RNA species, the $z$-axis values were set to be zero so as to remove the artifact peaks generated by juxtaposing data from two orthogonal LC methods.

## RESULTS

The overall strategy for developing the RNA purification method involved defining the parameters for the individual chromatographic elements for purification of ncRNA and then combining the two size-exclusion steps into a 2D system.

### 1D size-exclusion chromatography of eukaryotic and prokaryotic total RNA

Given the observation that virtually all classes of RNA, except mRNA, can be defined by their sequence lengths and molecular sizes, we coordinated two different size-range SEC columns to resolve total RNA. The 1D SEC of total cellular RNA has been used to separate small ncRNA (tRNA; 5S, 5.8S rRNA) from large ncRNA (16S, 18S, 23S, 26S rRNA), but large rRNA species were not resolved (21,22,32). We empirically tested several commercial SEC columns and found that two second-generation columns (Agilent Bio SEC-5 1000 Å pore size and Bio SEC-3 300 Å pore size) provided the best resolution after optimizing for temperature (60°C; evaluated range: ambient-70°C), eluent ionic strength (100 mM ammonium acetate; evaluated range: 8–250 mM) and flow rate (0.5 ml/min; evaluated range: 0.5–1 ml/min). Separations of total RNA from *E. coli* and human B lymphoblastic CCRF-SB cells on both columns are shown in Figure 1A–D. Baseline separation (resolution $R_s > 1.5$) of large rRNAs was achieved with the SEC-5 1000 Å column for both 23S and 16S rRNA from *E. coli* (Figure 1A), and for 28S and 18S rRNA from CCRF-SB (Figure 1B). Although low molecular weight (MW) rRNAs (5.8S, 5S), tRNA and smaller ncRNA eluted together on this column (Figure 1A and B), the SEC-3 300 Å column achieved resolution of tRNA from 5.8S/5S rRNA (Figure 1C and D).

For preparative size exclusion HPLC (SE-HPLC) isolations of RNA at microgram quantities, a fraction collector (Agilent 1260 FC-AS) is placed in-line after the detector. Fractions are collected by time segments, and the purity and integrity of each fraction were analyzed on an Agilent 2100 Bioanalyzer with appropriate RNA microfluidic chips (Supplementary Figure S1). For each fraction, mRNA and other non-canonical ncRNA species were not detected above the 50 pg/μl limit of detection of the RNA 6000 Pico (total RNA) and small RNA chips. For these small micro-fluidic separations, it is not always

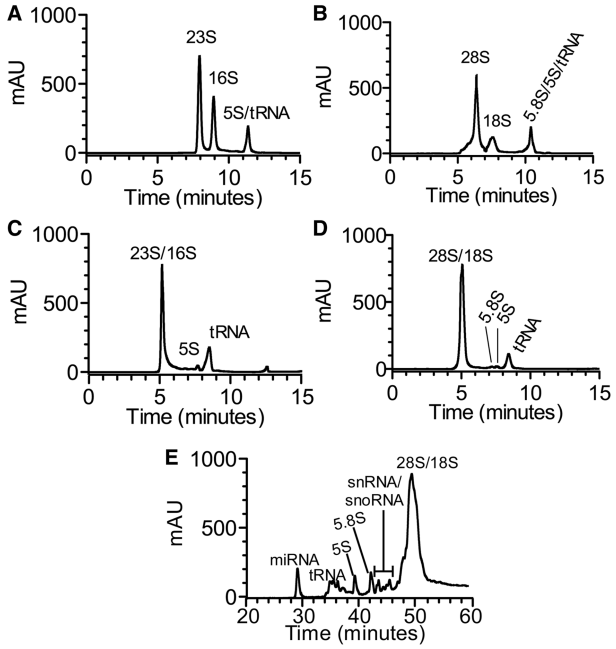


**Figure 1.** Separation of CCRF-SB and *E. coli* total RNA by SE-HPLC. (**A**) Typical profile of *E. coli* total RNA consisting of 23S, 16S rRNAs and co-eluting 5S rRNA and tRNA obtained on a Bio SEC-5 1000 Å column. (**B**) Typical profile of CCRF-SB total RNA consisting of 28S, 18S rRNAs and co-eluting 5.8S, 5S rRNA and tRNA obtained on a Bio SEC-5 1000 Å column. (**C**) Typical profile of *E. coli* total RNA consisting of 5S rRNA, tRNAs and co-eluting 16S and 23S rRNAs obtained on a Bio SEC-3 300 Å column. (**D**) Typical profile of CCRF-SB total RNA consisting of 5.8S, 5S rRNA, tRNAs and co-eluting 18S and 28S rRNAs obtained on a Bio SEC-3 300 Å column. The chromatograms show the analysis of 10 µg of total RNA extracted using Trizol reagent (Materials and Methods). (**E**) Separation of miRNA, tRNAs, 5.8S, 5S rRNAs, putative snRNAs and snoRNAs, and co-eluting 18S and 28S rRNAs from human lymphoblastic cell line CCRF-SB total RNA by IP RP HPLC obtained on a SOURCE 5RPC ST 4.5/150 column. The identity and purity of the RNAs collected in each fraction was validated with Bioanalyzer RNA 6000 Pico and Small RNA LabChips (Supplementary Figures S1 and S3).

possible to fully discern degradation products or co-purified RNA species with similar electrophoretic properties. The small fronting or tailing peaks observed in several of the electropherograms (Supplementary Figures S1D, S1G, S1H and S1L) may be attributed to these RNAs. Therefore, in these cases, we recommend a second purification using the same 1D SEC system with strict time segment cut-offs to improve the purity of the targeted RNA species.

Apart from miRNA and sRNAs, our isolation method allows recovery ≥80% for all other RNA species (Supplementary Figure S2A and B) on both SEC-3 300 Å and SEC-5 1000 Å columns. In addition, we observed no change in the linearity of the absorption isotherm for each targeted RNA species for up to 100 µg of injected total RNA (peak symmetries 1.0–1.4), with detector saturation at ~490 µg of total RNA injected. These parameters allow the user to optimize the injected load of RNA for purposes of recovery, purity or throughput. Equally important, we observed no volume overloading effects at sample volume injections up to 100 µl.

### 1D IP RPC for complete resolution of small RNA species

The IP RPC was used as the third dimension of separation to resolve all small ncRNA species, including 5S and 5.8S rRNA (18,33,34). Using a SOURCE 5RPC ST 4.5/150 column (5 µm particle size; 4.6 × 150 mm) and triethylammonium acetate (TEAA) for charge neutralization, we achieved complete resolution of small ncRNA from CCRF-SB human lymphoblast cells (Figure 1E), including separation of miRNA-sized fragments from tRNA and 5S from 5.8S rRNA. The size-based identity of these RNA species was verified by Bioanalyzer (Supplementary Figure S3). We observed multiple RNA peaks between 31 and 48 min (Figure 1E), which proved to be ~60–80 nt in apparent length by Bioanalyzer analysis (Supplementary Figure S3E). Given reports of sequence dependency in IP RPC single-stranded RNA separations (35), we believe that these peaks represent groups of tRNA isoforms. In addition, from 42 to 45 min (Figure 1E), another series of peaks with apparent lengths between 70 and 130 nt was observed (Supplementary Figure S3H), which match the size of several snoRNA and snRNA species (36). A final noteworthy feature of these studies is that baseline separation of 18S and 28S rRNA was achieved with SEC but not IP RPC (Figure 1A; Supplementary Figures S1G, S1H and S3B). Hence, the two complementary approaches provide complete resolution of all major ncRNA species.

We validated this chromatographic system for preparative isolations with RNA loads up to 40 µg of total RNA. At this scale, we recovered ≥70–80% of the targeted RNA species (Supplementary Figure S2C), with no significant loss of peak quality and resolution.

### 2D SEC design and validation with total RNA from *M. bovis* BCG

The results with 1D HPLC systems indicate that a 2D separation using both SEC-5 and SEC-3 columns would allow the complete resolution of most ncRNA under non-denaturing conditions, with the exception of 5S and 5.8S rRNA. To this end, we designed a valve-switching scheme that facilitates an online tandem SEC approach to the separation of total RNA (Supplementary Figure S4). In this non-orthologous 2D HPLC scheme, high MW RNA (> 500 kDa; e.g. 28S, 23S, 18S, 16S rRNA) is resolved on the SEC-5 column, whereas low MW RNA (<40 kDa; e.g. 5.8S/5S rRNA, tRNA, miRNA) is resolved on the SEC-3 column. When total cellular RNA is injected onto the SEC-5 column, high MW species are resolved from each other and from the retained low MW RNAs, which elute as a group directly onto the SEC-3 column where they are fractionated. Conversely, high MW RNA species separated on the SEC-5 column bypass the SEC-3 column and elute directly. This arrangement is completely modular and the column positions can be swapped while achieving the same level of separation, with the low MW RNA eluting before the high MW species. We performed 2D SEC on total RNA extracted from *M. bovis* BCG and separated its entire range of major ncRNA species within a single 40-min run (Figure 2A). Reproducible baseline separations were achieved for tRNA and 5S rRNA

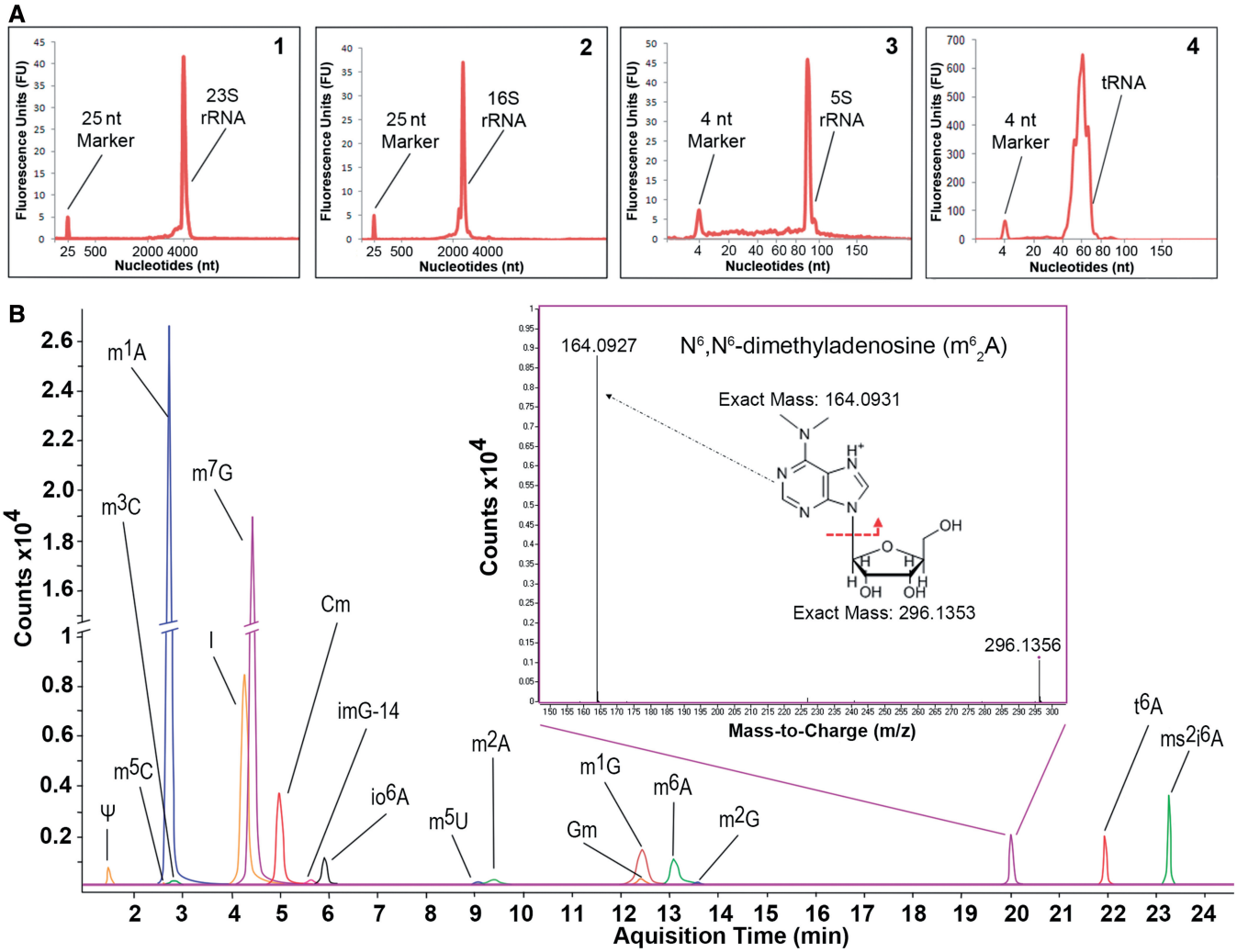


**Figure 2.** The 2D-SEC of BCG total RNA preserves the native post-transcriptional ribonucleoside modifications in purified tRNA. (**A**) Baseline separation of BCG total RNA to its component 23S (insert 1), 16S (insert 2), 5S rRNAs (insert 3) and tRNA (insert 4) obtained on a Bio SEC-5 1000 Å (column 1) and Bio SEC-3 300 Å (column 2) two-column online HPLC system (ID 7.8 mm, 300 mm for each column) demonstrating the purity and quality of each RNA species based on sequence lengths on the Bioanalyzer RNA 6000 Pico and Small RNA LabChips. (**B**) Extracted ion chromatograms of naturally occurring modified ribonucleosides in hydrolyzed BCG tRNA identified by HPLC-coupled triple quadrupole mass spectrometry in multiple reaction monitoring mode. The peaks of $m^1A$ (2.87 min) and $m^7G$ (4.53 min) are marked with '//' to indicate that they are in different scales from other peaks. Identities of the 18 post-transcriptional modifications detected are shown in Supplementary Table S2. Inset: MS/MS validation of $N^6,N^6$-dimethyladenosine ($m^6_2A$). Ribonucleoside with $m/z$ of 296.1356 was targeted for CID fragmentation on a high mass accuracy quadrupole time-of-flight mass spectrometer yielding a daughter ion with $m/z$ 164.0927.

($R_s = 4.4 \pm 0.1$), 5S rRNA and 16S rRNA ($R_s = 22 \pm 0.2$) and 16S rRNA and 18S rRNA ($R_s = 3.9 \pm 0.1$) for total RNA extracted from three independent BCG cultures. Additionally, the chromatography did not affect the spectrum or quantity of modified ribonucleosides in tRNA (Figure 3B; Supplementary Table S1), relative to our published values (31).

### Limitations of 2D SEC

To ascertain the biologically relevant exclusion limits of the 2D SEC platform, we performed studies covering the size range of 22–10 700 nt. Calibration curves with synthetic RNA MW markers (37) would not provide information about the exclusion and penetration limits for the columns for biological RNA species, given the presence of RNA secondary structures that affect the molecular dimensions and thus chromatographic behavior of biological RNA molecules. Therefore, we used viral RNA and 22 nt miRNA-like molecules to define the exclusion limits of the 2D system. We first spiked *in vitro* transcribed, full-length DENV vRNA measuring 10.7 kb into total RNA extracted from CCRF-SB cells. Although a separation with a resolution of 3.7 was achieved for 28S rRNA and vRNA using an Agilent SEC5 column (Supplementary Figure S5A), comparison of this chromatogram with that of DENV vRNA alone reveals a large tailing from the vRNA peak that spreads into the 28S rRNA peak. This implies that pure fractions of vRNA, but not 28S

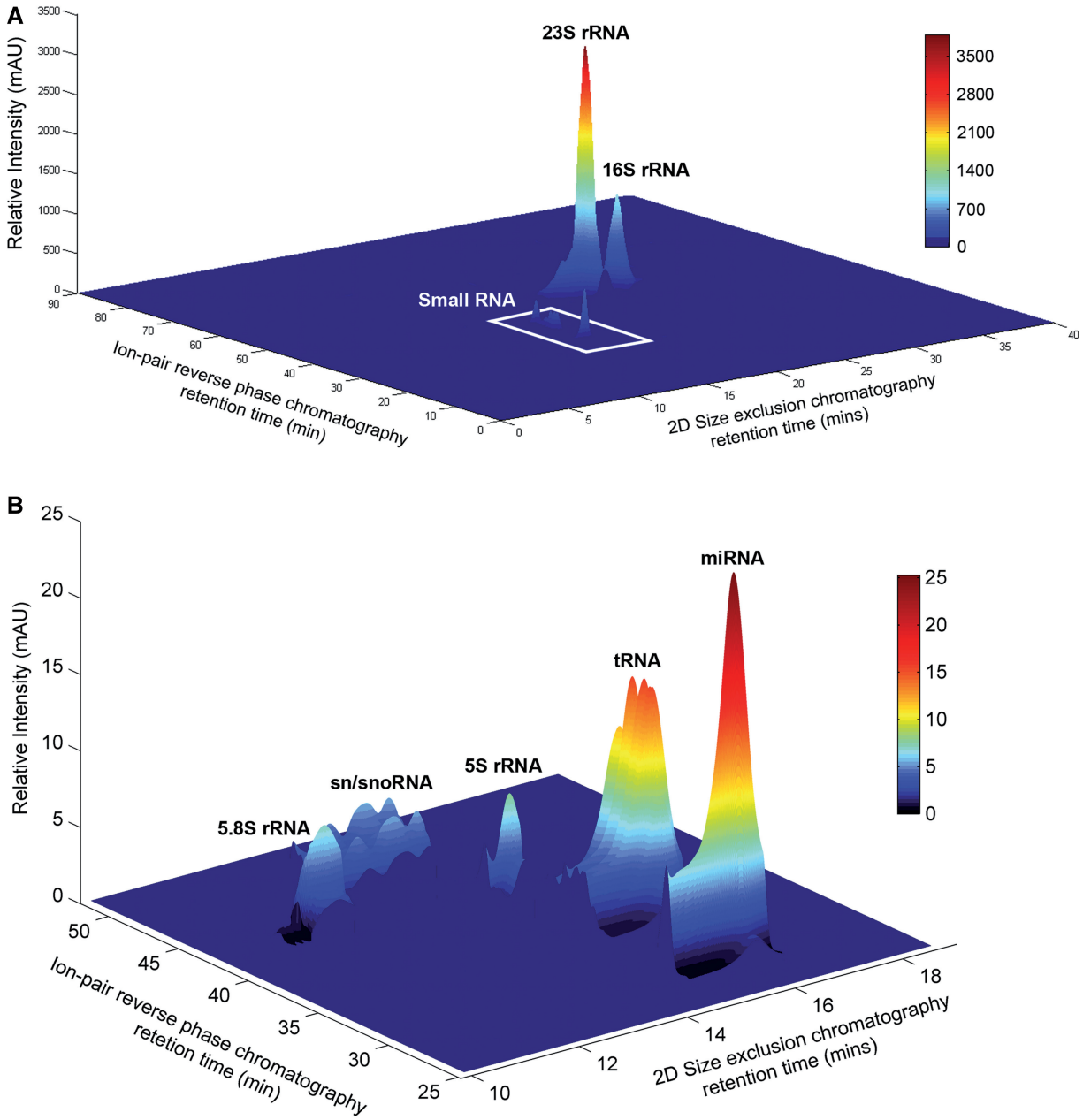


**Figure 3.** Reconstruction of the RNA landscape of Epstein-Barr virus-transformed TK6 cells by 2D SEC and IP RPC. (**A**) The 3D surface plot shows the analysis of 500 ng of total RNA extracted from TK6 cells using both 2D SEC (column 1: Bio SEC-3 300 Å; Column 2: Bio SEC-5 2000 Å) and IP RPC (SOURCE 5RPC ST 4.5/150). (**B**) Enhanced view of the smaller RNA species consisting of miRNA, tRNA, 5s and 5.8s rRNAs and putative snRNA and/or snoRNA. The identity and purity of the component RNA from orthographic projections of 2D SEC and IP RPC chromatograms is shown in Supplementary Figure S7.

rRNA can be purified from this mixture using the current 2D SEC setup. Similarly, to determine the biologically relevant penetration limit of the 2D SEC platform, we analyzed the resolution of a mixture of random 22 nt synthetic oligos, to simulate miRNA, and purified tRNA from CCRF-SB cells on an Agilent SEC3 column (Supplementary Figure S5B). Although a partial separation could be achieved between these two small ncRNA species, given the low cellular abundance of miRNA relative to tRNA, isolation of pure fractions of miRNA, solely based on SEC, would not be possible under these 2D SEC conditions. An additional IP RPC step could solve this problem (see Figure 1E).

To demonstrate the resolving power of this multidimensional (2D SEC, IP RPC) chromatographic approach to RNA purification, we reconstructed the RNA landscape of TK6 total RNA using the retention times of 2D SEC and IP RPC chromatograms to define spatial localizations on the X-Y plane and peak area as the *z*-axis (Figure 3A). As the relative intensities in the small RNA region are two orders-of-magnitude smaller than those of large ribosomal RNA, we rescaled this region in Figure 3B.

### Application of 2D SEC for isolation of *P. berghei* ncRNA from infected reticulocytes

To assess the resolving power of the HPLC platform, we applied it to the particularly challenging problem of separating host RNA species from those of an infecting microbial pathogen, using the example of ncRNA from malaria parasites infecting mammalian red blood cells. *P. berghei* is a protozoan parasite that causes malaria in rodents and is used as an *in vivo* disease model for human malaria (38). *Plasmodium berghei* preferably infects reticulocytes in which residual host RNA still exists. As a result, trace amounts of host RNA could contaminate preparations of *P. berghei* schizonts from lysed infected reticulocytes, as shown in Figure 4A. We injected total cellular RNA from purified *P. berghei* schizonts onto the 2D SEC system and resolved the variety of small and large ncRNA species (Figure 4B), with Bioanalyzer analysis of the fractions collected for each peak confirming the predicted length of the isolated RNA species (Supplementary Figure S6). In particular, pure fractions of tRNA, 5.8S rRNA and 5S rRNA were isolated, as well as putative snoRNA and snRNA species. We were able to completely resolve the unique ~800 nt partner of another ~3000 nt fragment that combines functionally to form the 28S rRNA of *P. berghei* (Figure 4A)(39,40). Baseline separation of the ~3000 nt 28S rRNA fragment and putative 18S rRNA was not achieved because of their close proximity in time (Figure 4B). In addition, no miRNA-length small RNA species were detected.

### Fluorometric quantification of purified RNA

Of the many commonly used spectroscopic methods for quantifying RNA, fluorescent RNA-binding dyes have proven to be highly sensitive and specific when a simple correction was applied for DNA contamination (41), and they avoid the problems of protein and DNA contamination associated with absorbance at 260 nm. However, the variety of secondary structures in different RNA species could affect the efficiency of fluorescence emission on dye binding and thus affect quantitative accuracy. To resolve this problem, we used the 2D HPLC platform to purify specific ncRNA species and then determined fluorescence correction factors for each type of RNA. Purified fractions of 28S rRNA, 18S rRNA and tRNA from CCRF-SB, and 23S rRNA, 16S rRNA and tRNA from *E. coli* DH5α were concentrated, desalted, qualitatively assessed (Bioanalyzer 6000 Nano LabChip) and quantified by absorbance at 260 nm. Following addition of Ribogreen dye, fluorescence emissions were quantified in dilutions of each RNA standard over concentrations ranging from 20–1000 ng/ml. As shown in Figure 5, there are significant differences in the fluorescence emission profiles of each of the ncRNA species when compared with a standard using total cellular RNA. Particularly, the fluorescence signal for RiboGreen increases by 10% for 28S rRNA compared with CCRF-SB total RNA, whereas it decreases by up to 11% for bacterial tRNA compared with *E. coli* total RNA (Supplementary Tables S2A, S2B). Thus, application of these weighting factors allows the use of readily purified total RNA from target cells as a standard for accurate quantification of a specific ncRNA using fluorescence dye assays.

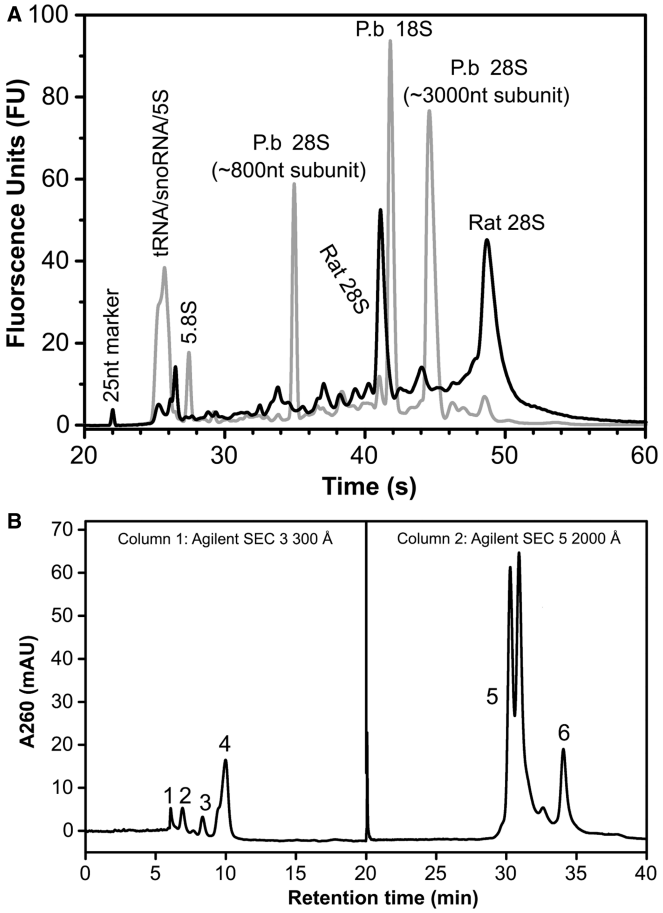


**Figure 4.** Isolation of ncRNA from *P. berghei*-infected rodent reticulocytes. (**A**) Bioanalyzer analysis of total RNA extracted from whole blood from uninfected rats (black line) and total RNA extracted from *P. berghei* schizonts purified from infected rat erythrocytes following lysis of the red blood cells and washing of the schizonts, as described in Supplementary Methods (gray lane). (**B**) 2D-SEC purification of *P. berghei* ncRNA. Total RNA from schizonts purified from lysed rodent reticulocytes was resolved on the 2D HPLC system, with Bio SEC-3 300 Å resolution of 5.8S rRNA (1), 5s rRNA (2), putative snRNA/snoRNA (3) and tRNA (4), and Bio SEC-5 1000 Å resolution of the 28s 800 nt rRNA fragment (6) from the co-eluting 18s rRNA and 28s 3000 nt rRNA fragment (5). Individual RNA species were collected from the 2-D HPLC elution, and the purity and identity of each fraction was evaluated by Bioanalyzer analysis as shown in Supplementary Figure S6.

## DISCUSSION

To facilitate the study of the chemistry and biology of ncRNA, we developed a multidimensional HPLC platform that reproducibly and efficiently purifies the major species of ncRNA across the complete size range up to 10 000 nt. This universal platform allows resolution, purification and quantification of ncRNA species in a cell under non-denaturing conditions and with post-transcriptional ribonucleoside modifications intact. The method was validated by purifying putative tRNA, small

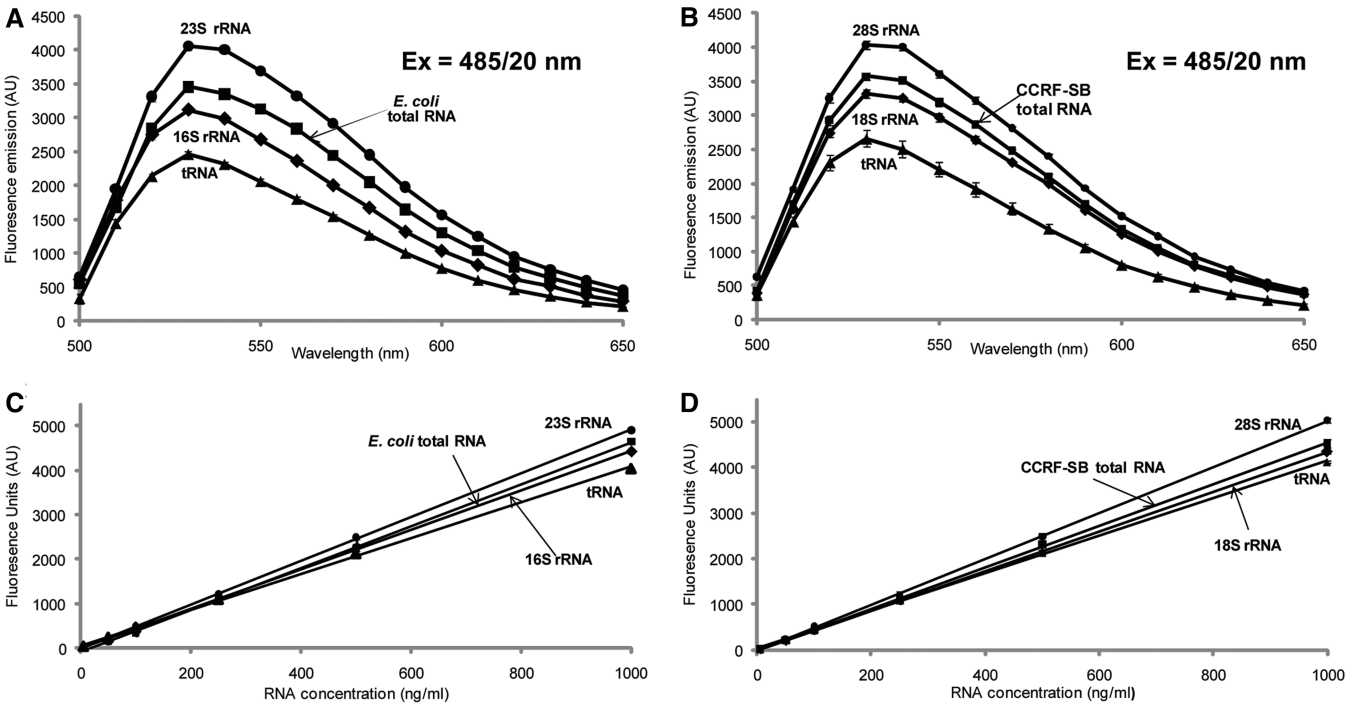


**Figure 5.** Fluorometric quantitation of purified RNA using RiboGreen with adjustments for species-specific responses. (**A**) Fluorescence enhancement of RiboGreen on binding to *E. coli* total RNA (black square) and HPLC purified *E. coli* 23S rRNA (black circle), 16S rRNA (black diamond) and tRNA (black triangle). (**B**) Fluorescence enhancement of RiboGreen on binding to CCRF-SB total RNA (black square) and HPLC purified CCRF-SB 28S rRNA (black circle), 18S rRNA (black diamond) and tRNA (black triangle). (**C**) RNA concentration curves of *E. coli* total RNA (black square) and HPLC purified *E coli* 23S rRNA (black circle), 16S rRNA (black diamond) and tRNA (black triangle). (**D**) RNA concentration curves of CCRF-SB total RNA (black square) and HPLC purified CCRF-SB 28S rRNA (black circle), 18S rRNA (black diamond) and tRNA (black triangle). The fluorescence of each RNA species with concentrations from 0 to 1000 ng/ml stained with RiboGreen was measured for fluorescence at 528/20 nm.

and large subunit rRNAs, and other small RNAs from *E. coli*, mycobacteria, human cells and plasmodium-infected rat reticulocytes, as well as *in vitro* transcribed, full-length viral RNA. As shown in Figure 3, the successful resolution of the major ncRNA species by the combined 2D SEC and IP RPC provides a complete picture of the RNA landscape within a cell or tissue and allows both sequencing of purified ncRNA and chemical interrogation of the pool of ncRNA species, such as an analysis of the stress-induced reprogramming of the spectrum of modified ribonucleosides in all ncRNA species in a cell (12,13,31).

This multidimensional chromatographic approach offers significant advantages over other methods for purifying ncRNA. Conventional preparative polyacrylamide gel electrophoresis is time-consuming ($\geq$2 d), denaturing and limited to RNA sizes <600 nt (42), with eluted RNA contaminated with acrylamide oligomers (15) and any dyes used to visualize the RNA. For purification of tRNA, denaturing (urea) polyacrylamide gels (43) have the advantage that larger amounts of RNA can be loaded into a single gel, with 1–3 mg of total RNA resolved on a 10% polyacrylamide gel (8 M urea) yielding 240 ± 60 ug of tRNA (13). With tRNA representing ~14% of total RNA in yeast (based on areas under the curve for UV absorbance signals from HPLC chromatograms), this yield of tRNA represents ~70% of input tRNA. However, this does not account for losses in subsequent removal of polyacrylamide fragments by filtration and/or purification by SEC HPLC. Similarly, agarose gels can be used for resolution and purification of larger RNAs (>600 nt)(44), with recovery by a variety of methods (45–48) that suffer from the same contamination problems. In contrast, RNA chromatography is faster, can be performed under non-denaturing conditions, uses simple solvent mobile phases that do not contaminate the sample and is more sensitive and easily automated for fraction collection (49).

The multidimensional chromatography platform developed here also has advantages over existing chromatographic methods that target individual ncRNA species (18,22,32,50). The newer Agilent SEC columns solve difficulties with the separation of large molecular weight rRNA observed in earlier work with RNA SEC (22,32). This limitation was only partially relieved in more recent efforts that use IP RPC for RNA separation (18,50). Conversely, purification of RNA species in the low MW size ranges (<100 nt) often requires an additional enrichment step either through the use of commercially available small RNA kits or with solid-phase extraction processes because of their low natural abundance and inefficiencies in extracting them with the commonly used acidic phenol chloroform method (51,52) without further enrichment on silica gel or glass fiber matrices (53). Although commercial systems such as LabChip XT (Caliper) and Pippin Prep (Sage Science) have recently been developed for size fractionation of DNA and analysis of quality of cDNA, an

equivalent system for the analysis and separation of RNA that covers the entire range of biologically relevant lengths is not available.

We solved these technical problems using multidimensional HPLC. By coupling two different SEC columns, together with a comprehensive offline IP RPC column, we were able to purify all major ncRNA species from miRNA to large 28s rRNA from a single batch of total RNA. The system was also capable of purifying viral genomic RNA intact from the host cell mixture of ncRNA. Interestingly, we were able to purify miRNA from CCRF-SB and TK6 B lymphoblast cell lines but not from *P. berghei*-infected rat reticulocytes, which is consistent with recent work, suggesting that plasmodium parasites do not express miRNA (54). These results demonstrate the utility of this HPLC platform for analysis and purification of the various ncRNA species within a cell. The sequences of the isolated RNA species can be collaborated with their genomic sequences by either RNA-seq or northern blotting. It is also important to point out that, although 2D chromatography provides the most efficient means to purify individual RNA species, the individual 1D HPLC systems can be used separately to achieve the same results as the 2D system in the event that the 2D HPLC technology is not available.

As with other chromatographic methods, the major limitation of this HPLC approach to RNA purification lies in the contamination of specific ncRNA fractions with similarly sized degradation products from larger RNA species. The problem presented by such contamination is illustrated with the analysis of modified ribonucleosides in RNA. For example, the nucleoside $m_2^6A$ has been identified in the 16S and 23S rRNA of archaea and bacteria and the 18S rRNA of eukarya, but never in tRNA. However, we recently identified $m_2^6A$ as an abundant modified ribonucleoside in tRNA from BCG (31), which raised the question of rRNA contamination of the tRNA fraction. The $m_2^6A$ was not detected in HPLC-purified tRNA from yeast, rat liver and human cells, which partially ruled out contamination with rRNA fragments (31), and Bioanalyzer analysis further confirmed a lack of degradation of rRNA in all of the samples (31). Along with such comparative analysis, contamination of small RNA fractions with fragments from larger RNA species can be assessed by RNA sequencing methods (55,56) and can potentially be removed by repurification of RNA fractions by an orthogonal chromatographic system that provides another basis for separating the contaminating RNA species, such as SEC-purified tRNA analyzed on IP RPC.

Another critical parameter for many applications of purified ncRNA species involves accurate quantification of the isolated RNA. For example, analysis of stress-induced reprogramming of modified ribonucleosides in tRNA (12,13,31) requires highly accurate quantification of input tRNA to control variance and allow meaningful comparisons of small changes. Our observation of variable emission spectra when RiboGreen is bound to different purified ncRNA species illustrates the impact of RNA composition on fluorescence-based quantification methods. Interestingly, it has been reported that PicoGreen, a related dye used for DNA quantitation, yields divergent fluorescence emissions when bound to genomic DNA from different organisms (57). To obviate the host of structure- and sequence-based causes of this discrepancy (58–60), we took the pragmatic approach of empirically characterizing fluorescent emission for many types of ncRNA and presenting the data as correction factors (Supplementary Table S1) for the major ncRNAs in *E. coli* and human cells (CCRF-SB) when using total cellular RNA as the calibration standard.

Among the most obvious applications for this RNA purification method are targeted RNA sequencing, characterization of modified ribonucleosides, purification of novel RNA species and analysis of viral RNA genomes (61). Targeted purification of RNA is essential for structural and functional characterization of novel RNA species, such as the large number of regulatory long ncRNA (62). The functional forms of these ncRNA after post-transcriptional processing events can then be correlated with their genomic sequences (63,64). The resulting enrichment for a specific transcript increases the sequencing power and efficiency for rare variants (65). Purification of individual ncRNA species is also critical for identifying and quantifying the dozens of chemically modified ribonucleosides incorporated post-transcriptionally into both coding (5) and ncRNA (10) species as part of the mechanism of translational control of cell response (12,13). The analysis of viral RNA genomes would also be aided by the ability to purify the virus RNA free from host RNA species. For example, it was recently discovered that the 11 kb RNA genome of the dengue virus is subject to adenosine methylation (61), which warrants purification of the viral RNA for analysis of other modified ribonucleosides. Hence, this platform provides a general strategy for preparing RNA for large-scale sequencing and composition analysis, and for downstream functional elucidation projects.

## SUPPLEMENTARY DATA

Supplementary Data are available at NAR Online.

## ACKNOWLEDGEMENTS

The authors thank Min Zin Oo (Singapore-MIT Alliance for Research and Technology) for providing the CCRF-SB cell line.

## FUNDING

Singapore-MIT Alliance for Research and Technology (to P.C.D.); and US National Institute of Environmental Health Sciences [NIEHS; ES017010 and ES002109]; A portion of the chromatography was performed in the NIEHS-supported Bioanalytical Facilities Core of the MIT Center for Environmental Health Sciences; SMA3 Graduate Fellowships (to Y.H.C. and C.S.N.). Funding for open access charge: This publication is made possible by the Singapore National Research Foundation under its Singapore-MIT Alliance for Research and Technology

research enterprise. The views expressed herein are solely the responsibility of the authors and do not necessarily represent the official views of the Foundation.

*Conflict of interest statement*. None declared.

## REFERENCES

1. Lujambio,A. and Lowe,S.W. (2012) The microcosmos of cancer. *Nature*, **482**, 347–355.
2. Bernstein,E. and Allis,C.D. (2005) RNA meets chromatin. *Genes Dev.*, **19**, 1635–1655.
3. Galasso,M., Elena Sana,M. and Volinia,S. (2010) Non-coding RNAs: a key to future personalized molecular therapy? *Genome Med.*, **2**, 12.
4. Dominissini,D., Moshitch-Moshkovitz,S., Schwartz,S., Salmon-Divon,M., Ungar,L., Osenberg,S., Cesarkas,K., Jacob-Hirsch,J., Amariglio,N., Kupiec,M. *et al.* (2012) Topology of the human and mouse m6A RNA methylomes revealed by m6A-seq. *Nature*, **485**, 201–206.
5. Jia,G., Fu,Y., Zhao,X., Dai,Q., Zheng,G., Yang,Y., Yi,C., Lindahl,T., Pan,T., Yang,Y.G. *et al.* (2011) N6-methyladenosine in nuclear RNA is a major substrate of the obesity-associated FTO. *Nat. Chem. Biol.*, **7**, 885–887.
6. Jahn,C.E., Charkowski,A.O. and Willis,D.K. (2008) Evaluation of isolation methods and RNA integrity for bacterial RNA quantitation. *J. Microbiol. Methods*, **75**, 318–324.
7. Anderson,A.C., Scaringe,S.A., Earp,B.E. and Frederick,C.A. (1996) HPLC purification of RNA for crystallography and NMR. *RNA*, **2**, 110–117.
8. Perez-Novo,C.A., Claeys,C., Speleman,F., Van Cauwenberge,P., Bachert,C. and Vandesompele,J. (2005) Impact of RNA quality on reference gene expression stability. *Biotechniques*, **39**, 52, 54, 56.
9. Sharp,P.A. (2009) The centrality of RNA. *Cell*, **136**, 577–580.
10. Phizicky,E.M. and Hopper,A.K. (2010) tRNA biology charges to the front. *Genes Dev.*, **24**, 1832–1860.
11. Li,M., Wang,I.X., Li,Y., Bruzel,A., Richards,A.L., Toung,J.M. and Cheung,V.G. (2011) Widespread RNA and DNA sequence differences in the human transcriptome. *Science*, **333**, 53–58.
12. Chan,C.T., Dyavaiah,M., DeMott,M.S., Taghizadeh,K., Dedon,P.C. and Begley,T.J. (2010) A quantitative systems approach reveals dynamic control of tRNA modifications during cellular stress. *PLoS Genet.*, **6**, e1001247.
13. Chan,C.T., Pang,Y.L., Deng,W., Babu,I.R., Dyavaiah,M., Begley,T.J. and Dedon,P.C. (2012) Reprogramming of tRNA modifications controls the oxidative stress response by codon-biased translation of proteins. *Nat. Commun.*, **3**, 937.
14. Wyatt,J.R., Chastain,M. and Puglisi,J.D. (1991) Synthesis and purification of large amounts of RNA oligonucleotides. *Biotechniques*, **11**, 764–769.
15. Lukavsky,P.J. and Puglisi,J.D. (2004) Large-scale preparation and purification of polyacrylamide-free RNA oligonucleotides. *RNA*, **10**, 889–893.
16. Seong,B.L. and RajBhandary,U.L. (1987) *Escherichia coli* formylmethionine tRNA: mutations in GGGCCC sequence conserved in anticodon stem of initiator tRNAs affect initiation of protein synthesis and conformation of anticodon loop. *Proc. Natl Acad. Sci. USA*, **84**, 334–338.
17. Easton,L.E., Shibata,Y. and Lukavsky,P.J. (2010) Rapid, nondenaturing RNA purification using weak anion-exchange fast performance liquid chromatography. *RNA*, **16**, 647–653.
18. Waghmare,S.P., Pousinis,P., Hornby,D.P. and Dickman,M.J. (2009) Studying the mechanism of RNA separations using RNA chromatography and its application in the analysis of ribosomal RNA and RNA:RNA interactions. *J. Chromatogr. A*, **1216**, 1377–1382.
19. Likic,S., Rusak,G. and Krajacic,M. (2008) Separation of plant viral satellite double-stranded RNA using high-performance liquid chromatography. *J. Chromatogr. A*, **1189**, 451–455.
20. Kim,I., McKenna,S.A., Viani Puglisi,E. and Puglisi,J.D. (2007) Rapid purification of RNAs using fast performance liquid chromatography (FPLC). *RNA*, **13**, 289–294.
21. Parvez,H., Kato,Y. and Parvez,S. (1985) *Gel Permeation and Ion-Exchange Chromatography of Proteins and Peptides*. VNU Science Press, Utrecht, The Netherlands.
22. Kato,Y., Sasaki,M., Hashimoto,T., Murotsu,T., Fukushige,S. and Matsubara,K. (1983) Operational variables in high-performance gel filtration of DNA fragments and RNAs. *J. Chromatogr.*, **266**, 341–349.
23. Batey,R.T. and Kieft,J.S. (2007) Improved native affinity purification of RNA. *RNA*, **13**, 1384–1389.
24. Miyauchi,K., Ohara,T. and Suzuki,T. (2007) Automated parallel isolation of multiple species of non-coding RNAs by the reciprocal circulating chromatography method. *Nucleic Acids Res.*, **35**, e24.
25. Cunningham,L., Kittikamron,K. and Lu,Y. (1996) Preparative-scale purification of RNA using an efficient method which combines gel electrophoresis and column chromatography. *Nucleic Acids Res.*, **24**, 3647–3648.
26. Wu,Q., Yuan,H., Zhang,L. and Zhang,Y. (2012) Recent advances on multidimensional liquid chromatography-mass spectrometry for proteomics: from qualitative to quantitative analysis—a review. *Anal. Chim. Acta*, **731**, 1–10.
27. Nagele,E., Vollmer,M., Horth,P. and Vad,C. (2004) 2D-LC/MS techniques for the identification of proteins in highly complex mixtures. *Expert Rev. Proteomics*, **1**, 37–46.
28. Zou,G., Chen,Y.L., Dong,H., Lim,C.C., Yap,L.J., Yau,Y.H., Shochat,S.G., Lescar,J. and Shi,P.Y. (2011) Functional analysis of two cavities in flavivirus NS5 polymerase. *J. Biol. Chem.*, **286**, 14362–14372.
29. Shi,P.Y., Tilgner,M., Lo,M.K., Kent,K.A. and Bernard,K.A. (2002) Infectious cDNA clone of the epidemic west nile virus from New York City. *J. Virol.*, **76**, 5847–5856.
30. Janse,C.J., Ramesar,J., van den Berg,F.M. and Mons,B. (1992) Plasmodium berghei: in vivo generation and selection of karyotype mutants and non-gametocyte producer mutants. *Exp Parasitol*, **74**, 1–10.
31. Chan,C.T., Chionh,Y.H., Ho,C.H., Lim,K.S., Babu,I.R., Ang,E., Wenwei,L., Alonso,S. and Dedon,P.C. (2011) Identification of N6,N6-dimethyladenosine in transfer RNA from *Mycobacterium bovis* Bacille Calmette-Guerin. *Molecules*, **16**, 5168–5181.
32. Uchiyama,S., Imamura,T., Nagai,S. and Konishi,K. (1981) Separation of low molecular weight RNA species by high-speed gel filtration. *J. Biochem.*, **90**, 643–648.
33. Azarani,A. and Hecker,K.H. (2001) RNA analysis by ion-pair reversed-phase high performance liquid chromatography. *Nucleic Acids Res.*, **29**, E7.
34. Noll,B., Seiffert,S., Vornlocher,H.P. and Roehl,I. (2011) Characterization of small interfering RNA by non-denaturing ion-pair reversed-phase liquid chromatography. *J. Chromatogr. A*, **1218**, 5609–5617.
35. Gilar,M., Fountain,K.J., Budman,Y., Neue,U.D., Yardley,K.R., Rainville,P.D., Russell,R.J. II and Gebler,J.C. (2002) Ion-pair reversed-phase high-performance liquid chromatography analysis of oligonucleotides: retention prediction. *J. Chromatogr. A*, **958**, 167–182.
36. Matera,A.G., Terns,R.M. and Terns,M.P. (2007) Non-coding RNAs: lessons from the small nuclear and small nucleolar RNAs. *Nat. Rev. Mol. Cell Biol.*, **8**, 209–220.
37. Wu,C.S. (2004) *Handbook of Size Exclusion Chromatography and Related Techniques*, 2nd edn. Marcel Dekker, New York.
38. Janse,C.J., Franke-Fayard,B., Mair,G.R., Ramesar,J., Thiel,C., Engelmann,S., Matuschewski,K., van Gemert,G.J., Sauerwein,R.W. and Waters,A.P. (2006) High efficiency transfection of *Plasmodium berghei* facilitates novel selection procedures. *Mol. Biochem. Parasitol.*, **145**, 60–70.
39. Dame,J.B. and McCutchan,T.F. (1983) The four ribosomal DNA units of the malaria parasite *Plasmodium berghei*. Identification, restriction map, and copy number analysis. *J. Biol. Chem.*, **258**, 6984–6990.
40. Dame,J.B., Sullivan,M. and McCutchan,T.F. (1984) Two major sequence classes of ribosomal RNA genes in *Plasmodium berghei*. *Nucleic Acids Res.*, **12**, 5943–5952.

41. Jones,L.J., Yue,S.T., Cheung,C.Y. and Singer,V.L. (1998) RNA quantitation by fluorescence-based solution assay: RiboGreen reagent characterization. *Anal. Biochem.*, **265**, 368–374.
42. Nilsen,T.W. (2013) Gel purification of RNA. *Cold Spring Harb. Protoc.*, **2013**, 180–183.
43. Barciszewska,M.Z., Krajewski,J., Gawronska,I. and Barciszewski,J. (1992) Rapid separation of tyrosine-specific tRNA from white lupin. *Acta Biochim. Pol.*, **39**, 223–226.
44. Brown,A.J. (1996) Preparation of total RNA. *Methods Mol. Biol.*, **53**, 269–276.
45. Duro,G., Izzo,V. and Barbieri,R. (1993) Methods for recovering nucleic acid fragments from agarose gels. *J. Chromatogr.*, **618**, 95–104.
46. Hammann,C. and Tabler,M. (1999) Quantitative recovery of nucleic acids from excised gel pieces by isotachophoresis. *Biotechniques*, **26**, 422–424.
47. Krowczynska,A.M., Donoghue,K. and Hughes,L. (1995) Recovery of DNA, RNA and protein from gels with microconcentrators. *Biotechniques*, **18**, 698–703.
48. Fremont,P., Dionne,F.T. and Rogers,P.A. (1986) Recovery of biologically functional messenger RNA from agarose gels by passive elution. *Anal. Biochem.*, **156**, 508–514.
49. Gjerde,D.T., Hoang,L. and Hornby,D. (2009) *RNA purification and analysis: sample preparation, extraction, chromatography*. Wiley-VCH, Weinheim.
50. Dickman,M.J. and Hornby,D.P. (2006) Enrichment and analysis of RNA centered on ion pair reverse phase methodology. *RNA*, **12**, 691–696.
51. Chomczynski,P. and Sacchi,N. (1987) Single-step method of RNA isolation by acid guanidinium thiocyanate-phenol-chloroform extraction. *Anal. Biochem.*, **162**, 156–159.
52. Chomczynski,P. and Sacchi,N. (2006) The single-step method of RNA isolation by acid guanidinium thiocyanate-phenol-chloroform extraction: twenty-something years on. *Nat. Protoc.*, **1**, 581–585.
53. Rio,D.C., Ares,M. Jr, Hannon,G.J. and Nilsen,T.W. (2010) Guidelines for the use of RNA purification kits. *Cold Spring Harb. Protoc.*, **2010**, pdb ip79.
54. Xue,X., Zhang,Q., Huang,Y., Feng,L. and Pan,W. (2008) No miRNA were found in *Plasmodium* and the ones identified in erythrocytes could not be correlated with infection. *Malar J*, **7**, 47.
55. Ozsolak,F. and Milos,P.M. (2011) RNA sequencing: advances, challenges and opportunities. *Nat. Rev. Genet.*, **12**, 87–98.
56. Ozsolak,F., Platt,A.R., Jones,D.R., Reifenberger,J.G., Sass,L.E., McInerney,P., Thompson,J.F., Bowers,J., Jarosz,M. and Milos,P.M. (2009) Direct RNA sequencing. *Nature*, **461**, 814–818.
57. Holden,M.J., Haynes,R.J., Rabb,S.A., Satija,N., Yang,K. and Blasic,J.R. Jr (2009) Factors affecting quantification of total DNA by UV spectroscopy and PicoGreen fluorescence. *J. Agric. Food Chem.*, **57**, 7221–7226.
58. Burns,V.W. (1971) Fluorescence polarization characteristics of the complexes between ethidium bromide and rRNA, tRNA, and DNA. *Arch. Biochem. Biophys.*, **145**, 248–254.
59. Horie,K., Wada,A. and Fukutome,H. (1981) Conformational studies of *Escherichia coli* ribosomes with the use of acridine orange as a probe. *J. Biochem.*, **90**, 449–461.
60. Chow,C.S. and Bogdan,F.M. (1997) A structural basis for RNA-ligand Interactions. *Chem. Rev.*, **97**, 1489–1514.
61. Dong,H., Chang,D.C., Hua,M.H., Lim,S.P., Chionh,Y.H., Hia,F., Lee,Y.H., Kukkaro,P., Lok,S.M., Dedon,P.C. *et al.* (2012) 2'-O methylation of internal adenosine by flavivirus NS5 methyltransferase. *PLoS Pathog.*, **8**, e1002642.
62. Rinn,J.L. and Chang,H.Y. (2012) Genome regulation by long noncoding RNAs. *Annu. Rev. Biochem.*, **81**, 145–166.
63. Mullineux,S.T. and Lafontaine,D.L. (2012) Mapping the cleavage sites on mammalian pre-rRNAs: where do we stand? *Biochimie*, **94**, 1521–1532.
64. Beier,H., Barciszewska,M., Krupp,G., Mitnacht,R. and Gross,H.J. (1984) UAG readthrough during TMV RNA translation: isolation and sequence of two tRNAs with suppressor activity from tobacco plants. *EMBO J.*, **3**, 351–356.
65. Levin,J.Z., Berger,M.F., Adiconis,X., Rogov,P., Melnikov,A., Fennell,T., Nusbaum,C., Garraway,L.A. and Gnirke,A. (2009) Targeted next-generation sequencing of a cancer transcriptome enhances detection of sequence variants and novel fusion transcripts. *Genome Biol.*, **10**, R115.